MECHANICAL PROPERTIES AND MICROSTRUCTURE OF MELT-SPUN SUPERALLOY RIBBONS

K. Yasuda, M. Tsuchiya, T. Kuroda and M. Suwa

Hitachi Research Laboratory Hitachi, Ltd.
Hitachi-shi, Ibaraki-ken, 317 Japan

Abstract

Rapid solidification is expected to produce fine grained superalloys displaying enhanced mechanical properties. The current paper describes the production of melt-spun ribbons of two nickel base superalloys (Rene' 80 and IN738LC) and a cobalt-base superalloy (FSX414). Their microstructures have been characterized by metallographic techniques, electrical resistivity changes and hardness measurements. Tensile properties were determined at ambient and elevated temperatures, where values of the strain rate sensitivity indicate that micrograin superplasticity may be occurring.

Introduction

Alloys produced by rapid quenching from the melt have demonstrated remarkable characteristics such as grain refinement, extended solid solution, the formation of metastable phases and metallic glasses. Superalloys, conventionally produced by lost wax investment casting, have been used for high temperature components in aircraft engines and gas turbines. Cast superalloys have intrinsic disadvantages, such as solute segregation, grain coarsening and casting defects. However, if their grains are made extremely fine by rapid quenching, the compositional segregation can be reduced or eliminated, thereby improving mechanical properties and allowing fine grain superplasticity to be utilized in their high temperature deformation.

There are two typical methods for rapid quenching: power production and the melt spinning of ribbons. Few papers have been published concerning the making of melt-spun ribbons and their basic characteristics. The purpose of the present study is to produce fine-grained ribbons of both nickel and cobalt base superalloys by double roller quenching and to investigate their mechanical properties and microstructures.

Method and Experimental Procedure

The alloys used in this study were two nickel-base superalloys (Rene' 80, IN738LC) and one cobalt-base superalloy (FSX414). Their chemical compositions are given in Table I. Melt-spun superalloy ribbons were made from their commercial master ingots by a double roller quenching apparatus. A small amount of alloy weighing about 10g was put into a quartz crucible and melted in a high-frequency induction furnace. The molten metal was ejected through an orifice of 0.8 or 1 mm diameter with the help of Ar overpressure and rapidly cooled between the two turning rollers. A Cu-2%Be alloy was used for the rollers because of its high thermal conductivity and hardness. The ribbons produced were 50-120 m in thickness, 5-10 mm in width and about 1500 mm in length. The chemical compositions of the ribbons given in Table I are nearly the same as those of their master ingots.

Table I Chemical compositions of superalloys (wt%)

		C	Si	Mn	P	S	Ni	Co	Cr	W	Mo	Ta	Al	Ti	B	Nb	Zr	Fe
Renē 80	Ingot	0.16	0.07	0.01	0.006	0.003	Bal.	9.51	13.94	4.06	3.90	—	2.96	5.02	0.0103	—	0.04	—
	Ribbon	0.17	0.08						13.94				2.94	5.05	0.0095		0.04	
IN738LC	Ingot	0.10	0.03	0.01	0.003	0.003	Bal.	8.63	15.99	2.52	1.71	1.85	3.32	3.38	0.056	0.84	0.08	—
	Ribbon	0.11	0.04						15.88				3.31	3.38	0.104		0.08	
FSX414	Ingot	0.24	0.92	0.40	0.009	0.009	10.88	Bal.	29.02	7.46	—	—	—	—	0.0051	—	—	0.93
	Ribbon	0.25	0.90						28.97						0.0046			

The tensile specimen shown in Figure 1 was cut from the ribbons by discharge machining and then ground on emery paper to remove surface contamination. Tensile tests were conducted at ambient and high temperatures (900°C, 950°C) using an Instron type tensile test machine. The strain rate was controlled by changing the initial crosshead speed. Superplastic potential was evaluated in terms of the strain rate sensitivity, "m", which is defined by the following equation: $\sigma = K\dot{\varepsilon}^{m}$, where σ; flow stress, $\dot{\varepsilon}$; strain rate, K; constant. Optical microscopy, scanning electron microscopy (SEM) and transmission electron microscopy (TEM) were used to characterize the microstructure of the ribbons. Furthermore, the precipitation behavior was monitored by electrical resistivity measurement at liquid nitrogen temperature.

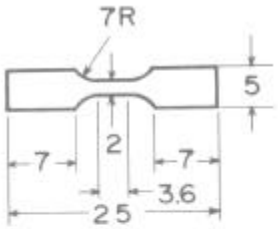

Figure 1 Tensile test specimen

Results and Discussion

Rene' 80 ribbons produced by the double roller quenching are shown in Figure 2. It has been reported that both the width and the thickness of melt-spun ribbons are affected by roll surface velocity and nozzle orifice diameter (1). With increasing roll surface velocity, the width and thickness decrease. The effects of the surface velocity together with nozzle orifice diameter on the width and thickness of the Rene' 80 ribbons are shown in Figure 3 and Figure 4, respectively. Figure 5 shows the scanning electron micrograph of the cross-section perpendicular to the Rene' 80 ribbon's length direction. Fine columnar structure is seen to extend inward from both surfaces of the ribbon, leaving the final solidified region near the centerline. The secondary dendrite arm spacing of all the superalloys was about 0.5 μm. According to Mehrabian's relationship between the dendrite arm spacing and the superalloy ribbon cooling rate (2), the cooling rates of the ribbons in the present study are estimated to be $5 \times 10^4 \sim 5 \times 10^5$ K/s.

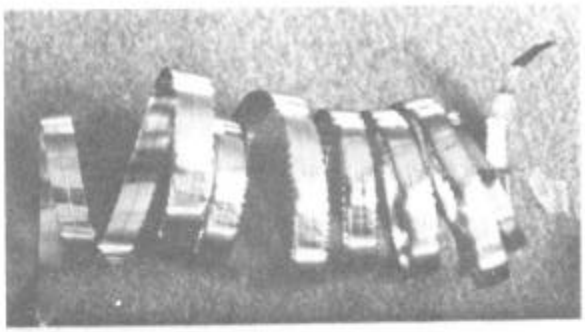

Figure 2 Rene80 ribbons produced by the double roller quenching

The transmission electron micrographs of the quench rolled Rene' 80, IN738LC and FSX414, as seen in Figure 6, show fine structures with a cell size of about 1 μm, which cannot be produced by conventional solidification processes. Fine grain sizes and high angle boundaries are considered microstructural requirements for superplasticity (3). Figure 7 shows the transmission electron micrograph of a quench rolled IN738LC ribbon. The crystallographic plane of, for instance, the grain indicated as No. 1 is (013). The adjacent grain boundary indicated by No. 2 exhibits the same plane (013) after tilting the specimen at an angle of 30° to the plane vertical to the incident electron beam. This observation suggests that the interface between the No. 1 and the No. 2 grains is a high angle tilt grain boundary. As clearly seen in Figure 7, the No. 1 grain consists of several cells, whose boundaries are presumably low angle boundaries. Similar observations were also made on the Rene' 80 and FSX414 ribbons.

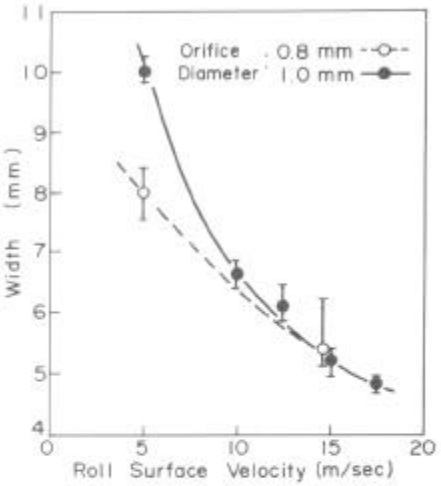

Figure 3 Effects of the roll surface velocity and nozzle orifice diameter on the width of Renē80 ribbons

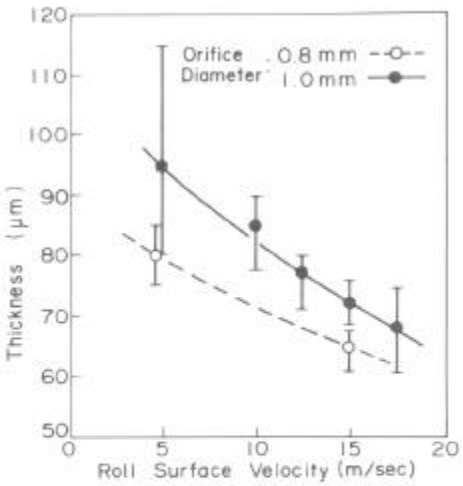

Figure 4 Effects of the roll surface velocity and nozzle orifice diameter on the thickness of Renē80 ribbons

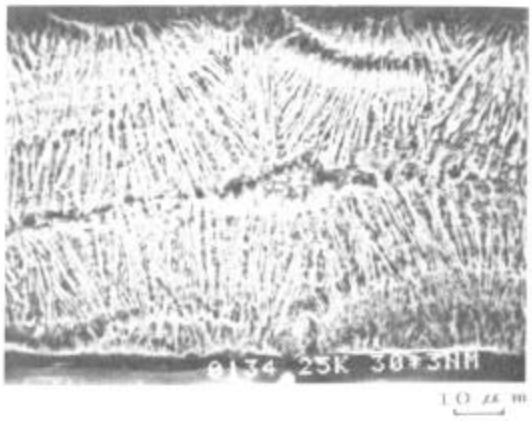

Figure 5 Scanning electron micrograph of the cross-section perpendicular to the Renē80 ribbon's length direction

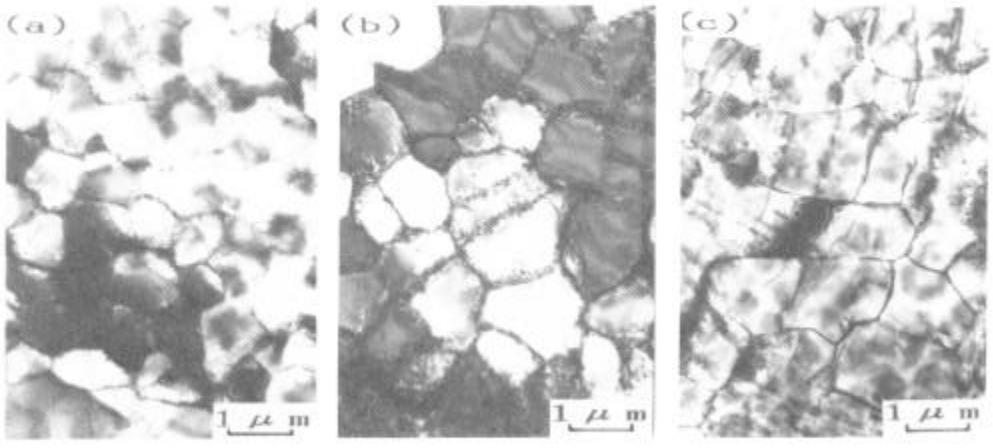

Figure 6 Transmission electron micrographs of the quench rolled ribbons (a): Renē80, (b): IN738LC, (c): FSX414

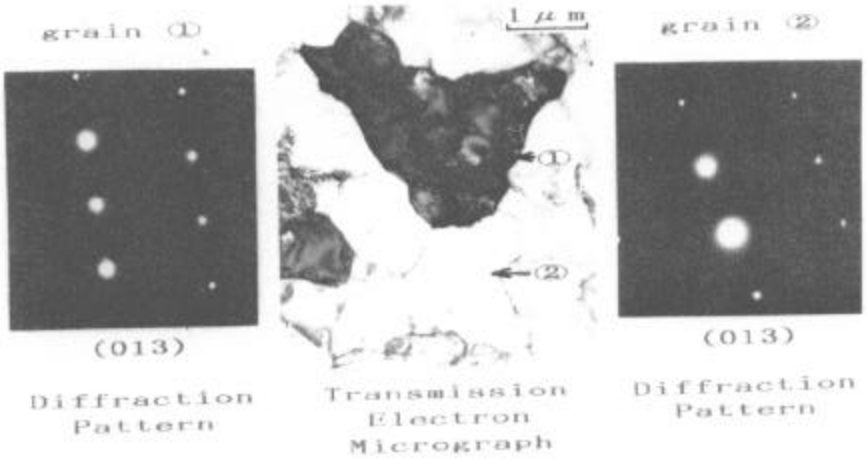

Figure 7 Transmission electron micrograph of the quench rolled IN738LC ribbons

Figure 8 shows the resistivity measured at liquid nitrogen temperature and also the hardness of the ribbons after aging at temperatures from 400°C to 1000°C for 1 h. In the range of 500°C to 700°C, the resistivity increases on aging, showing a maximum at 600°C. Increases in resistivity during the early stages of precipitation have been reported in most precipitation-hardening alloys as cluster zones (precipitate embryos) form. When the size of these cluster zones grows to 1 mm, nearly equal to the wave length of the conducting electron, the resistivity increases because of an increase in conducting electron scattering (4). The peak in resistivity (600°C) is thought to correspond to the formation of cluster zones of that size, whereas the peak in hardness (850°C) is thought to result from the further growth of these zones.

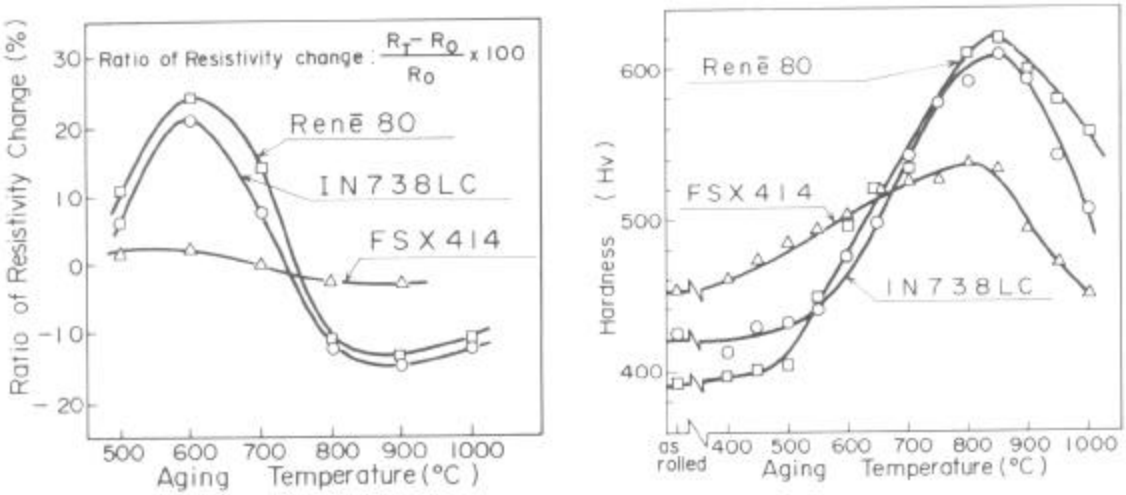

Figure 8 Electrical resistivity change and hardness change during isochronal aging (400°C - 1000°C). Ro: resistivity of quench rolled specimen, R: resistivity of specimen aged at T (°C)

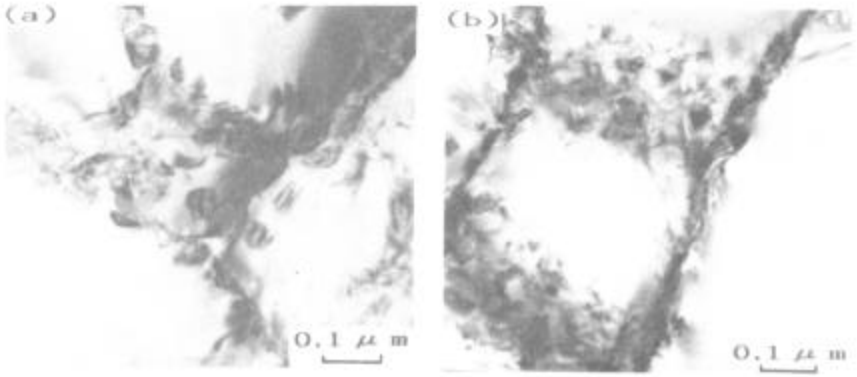

Figure 9 Transmission electron micrographs at grain boundaries and their surroundings in the Rene80 ribbon (a): as quench rolled, (b): aged at 600°C for 1h.

Figure 9 shows transmission electron micrographs both at grain boundaries and their surroundings in a Rene' 80 ribbon. In the quench rolled specimen (Figure 9(a)), irregular grain boundaries are revealed with no precipitates in the grains. The shape of these grain boundaries is assumed to be due to the formation of fine precipitates coupled with strains generated during solidification. The pinning apparently remains even after 600°C aging, as seen in Figure 9(b), and completely disappears only after 900°C aging. The fine precipitates at grain boundaries were identified as TiC by electron diffraction and energy dispersive X-ray analysis.

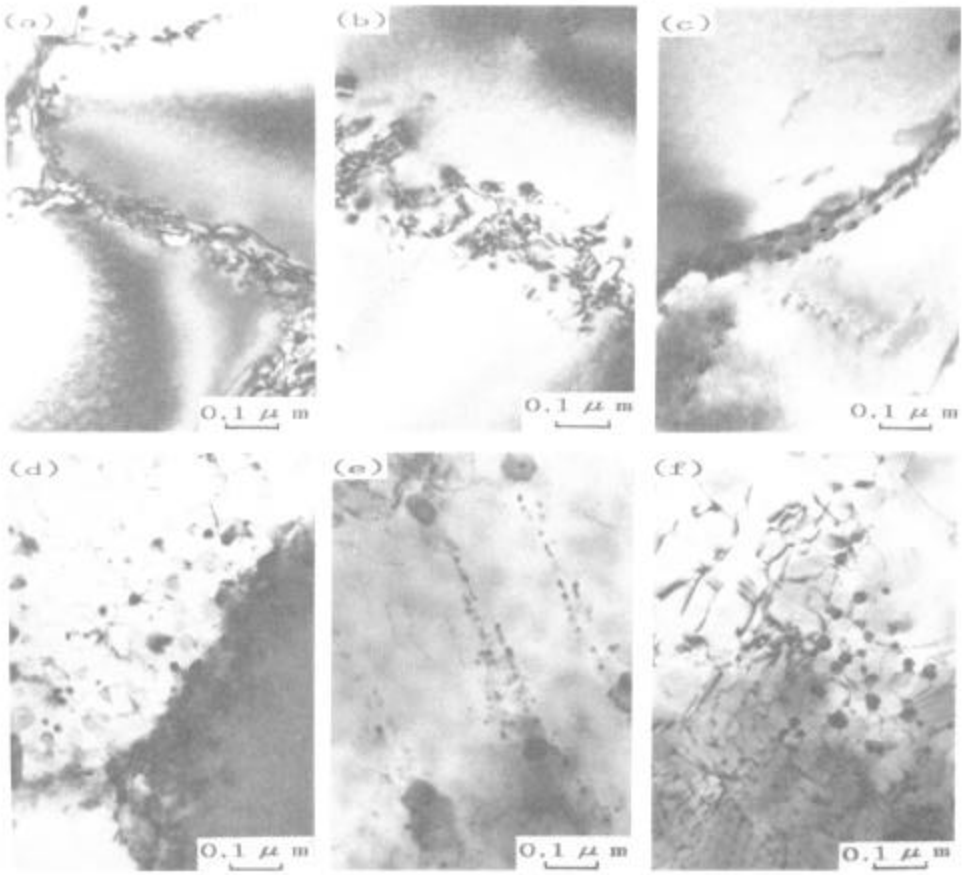

Figure 10 TiC carbide in the IN738LC ribbons (a): as quench rolled, (b): 600°C × 1h, (c): 700°C × 1h, (d): 800°C × 1h, (e): 900°C × 1h, (f): 1000°C × 1h.

MC carbide precipitation was also observed in the IN738LC ribbons, as shown in Figure 10. MC carbide forms only at grain boundaries in the quenched specimens. Upon aging at 800°C and above for 1 h, MC begins to form within the grains. The precipitates at grain boundaries in the Rene' 80 ribbon aged at 800°C for 1 h were identified as $Cr_{23}C_6$ by electron diffraction and composition analysis. In addition to $Cr_{23}C_6$ carbides, M_6C carbides containing Mo and W were also found in the Rene' 80 ribbon. This M_6C was not observed in the IN738LC ribbon because of its lower W and Mo contents.

The intergranular precipitation sequence in the Rene' 80 ribbon is shown in Figure 11. Few clearly resoluble precipitates were present until after aging at temperatures above 400°C. After aging at 700°C for 1 h the diffraction pattern indicates the presence of γ'. No indication of this phase was found at 600°C. With increasing aging temperature larger γ' precipitates are found. Figure 12 summarizes the precipitation sequences in IN738LC and Rene' 80.

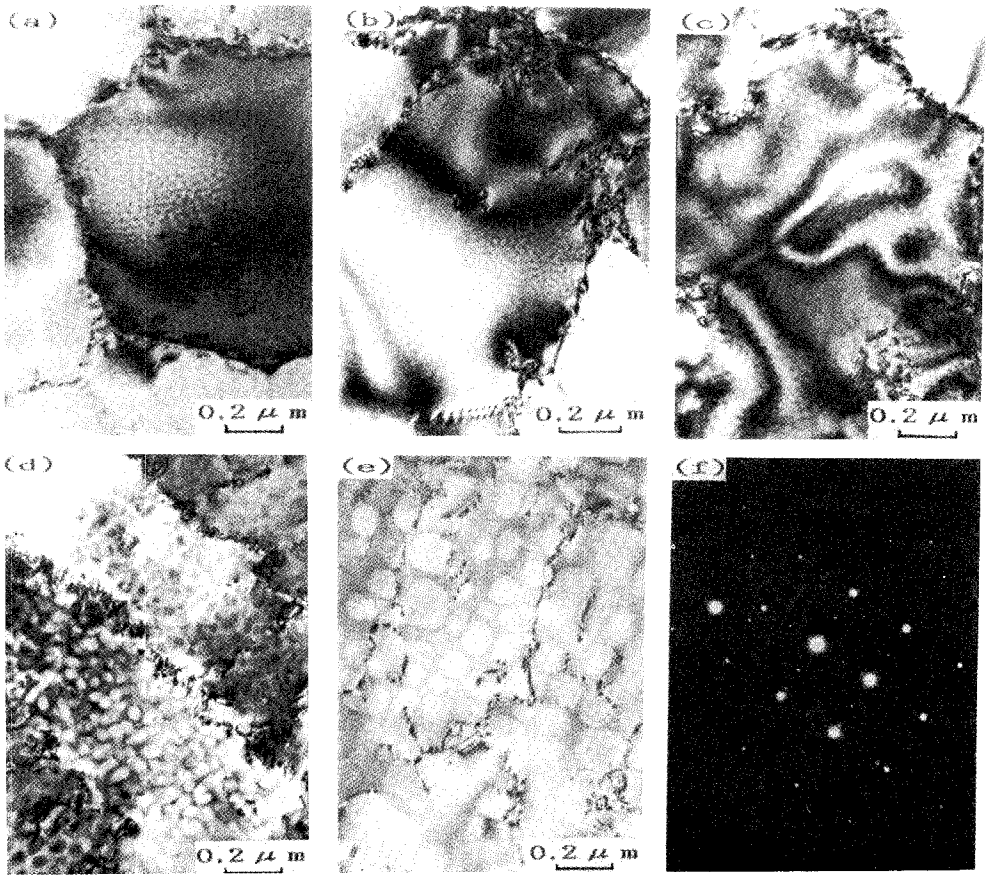

Figure 11 Precipitation morphology in the Rene80 ribbons aged for 1h. (a); as quench rolled, (b); 400°C, (c); 700°C, (d); 900°C, (e); 1000°C, (f); diffraction pattern from (c)

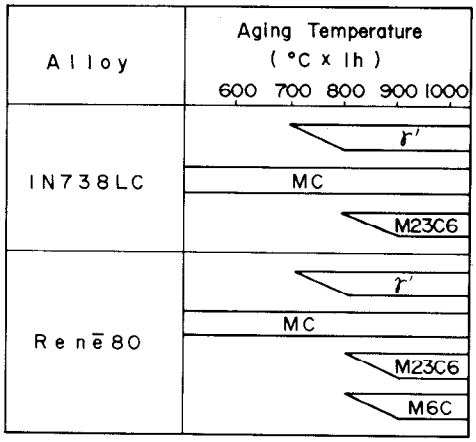

Figure 12 Precipitation sequence for the IN738LC and the Renē80 ribbons

The microstructure of the FSX414 ribbon is shown in Figure 13. There is a distinct difference between its $Cr_{23}C_6$ carbide morphology and that found in conventional castings. In the as quench rolled specimen (Figure 13(a)), no precipitate is found in the grains and only a small amount of $Cr_{23}C_6$ carbide at the grain boundaries. Furthermore, there is no evidence of precipitation of eutectic $Cr_{23}C_6$ carbide which is commonly found in the conventionally cast FXS414. As the aging temperature is increased, precipitates begin to form mainly at the grain boundary triple points. These precipitates were identified as $Cr_{23}C_6$ by electron diffraction.

Mechanical properties were measured both at ambient and high temperatures (900°C, 950°C). Table II shows the tensile properties at room temperature of the quench rolled ribbons. Tensile strengths and elongations are higher than those found in conventional castings. These improvements are attributed mainly to the formation of fine grain structures in the ribbons.

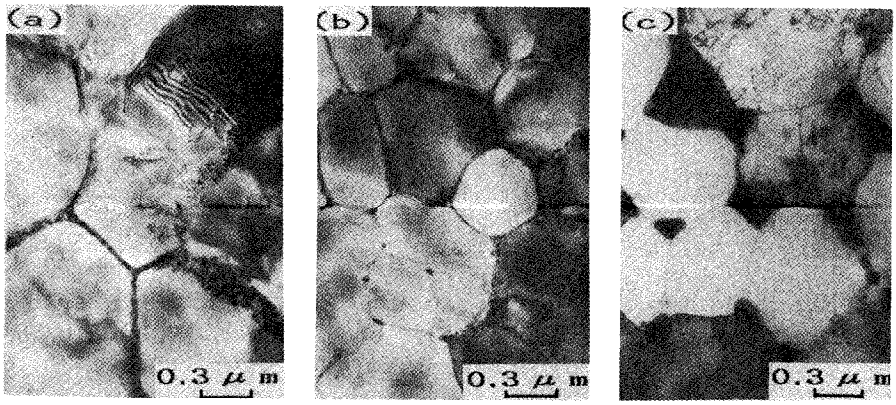

Figure 13 Microstructure of FSX414 ribbons (a); as quench rolled, (b); 600°C × 1h, (c); 1000°C × 1h

Table II Tensile properties at room temperature

Alloy	Process	Tensile Strength (MPa)	Elongation (%)
Renē 80	Melt-Spinning (Ribbon)	1107 ~ 1127	10 ~ 14
	Conventional Cast	1102 ~ 1112	5 ~ 6
IN738LC	Melt-Spinning (Ribbon)	1127 ~ 1176	15 ~ 25
	Conventional Cast	1087 ~ 1127	5 ~ 8
FSX414	Melt-Spinning (Ribbon)	1323 ~ 1401	31 ~ 35
	Conventional Cast	823 ~ 832	15 ~ 16

The tensile strengths at high temperatures as a function of strain rate are shown in Figure 14. The strain rate sensitivity, m, is also indicated. The m value for IN738LC tested at 900°C and 950°C is calculated to be 0.52. In the Rene' 80 ribbons, the m value is somewhat less but increases when the testing temperature is raised from 900°C to 950°C. On the other hand, the m value of the FSX414 ribbon is low compared with those of the IN738LC and the Rene' 80 ribbons.

As m values above 0.3 are considered a prerequisite for superplasticity, it may well be that the IN738LC and Rene' 80 ribbons would exhibit this phenomenon. It is thought that the lower m values found in the FSX414 result from the large $Cr_{23}C_6$ carbides formed at triple points which could suppress the grain boundary sliding needed for superplastic properties. It may be possible to produce higher m values in the FSX414 ribbons by controlling the carbide morphology through heat treatment or chemistry modification.

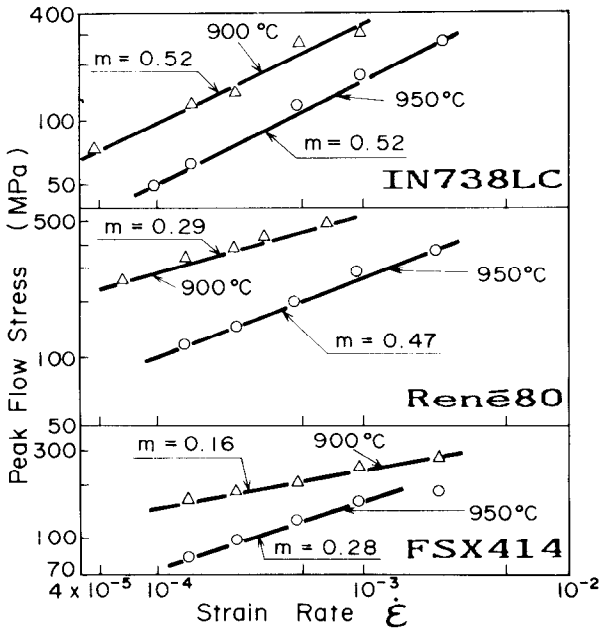

Figure 14 Tensile properties at high temperature, correlation between $\log\sigma$ and $\log\dot{\varepsilon}$ of quench rolled ribbons.

Conclusions

1) Fine grain Rene' 80, IN738LC and FSX414 superalloy ribbons can be produced by double roller quenching technique. The ribbons produced by this method exhibited columnar structures with about 1 m cell sizes.

2) Electrical resistivity measurement was found to be an effective means of monitoring precipitation. In this manner, electrical resistivity changes could be correlated with hardness change in the superalloy ribbons.

3) In the nickel-base superalloy ribbons, TiC carbide probably forms at grain boundaries during solidification. $Cr_{23}C_6$ carbide was found to form at grain boundaries after aging at about 800°C and above both in the Rene' 80 and in the IN738LC ribbons. M_6C carbide containing Mo and W was found to precipitate at grain boundaries only in the Rene' 80. Clearly visible γ' precipitates were revealed in both alloys when aged at 700°C and above.

4) In the cobalt-base superalloy (FSX414), no eutectic carbide was found, and only a small amount of $Cr_{23}C_6$ carbide was present at grain boundaries in the quench rolled ribbon. Upon subsequent aging, $Cr_{23}C_6$ tended to precipitate mainly at the grain boundary triple points.

5) Room temperature tensile properties of the superalloy ribbons were superior to those of conventional cast superalloys. This improvement is thought to result from the fine grain structures in the ribbons. High values of the strain rate sensitivity index were found in the nickel-base superalloy ribbons but not in the cobalt-base superalloy ribbons. This behavior is explained in terms of the different precipitate morphologies observed.

Acknowledgements

This work was performed under management of Research and Development Institute of Metals and Composites for Future Industries as a part of the R & D Project of Basic Technology for Future Industries sponsored by Agency of Industrial Science and Technology, MITI.

References

(1) K. Miyazawa, T. Choh and M. Inoue: "Rolling Characteristics in the Twin-Roll Rapid Solidification Process", Trans. of the Japan Inst. of Metals, 14, 11 (1983), pp. 781-788.

(2) R. Mehrabian: "Relationship of Heat Flow to Structure in Rapid Solidification Processing", Proc. Int. Conf. on Rapid Solidification Processing, Reston, Va, U.S.A., Nov 13-16, (1977), pp. 9-27.

(3) O.D. Sherby, R.D. Caligiuri, E.S. Kayali, and R.A. White: "Fundamentals of Superplasticity and its Application", Proc. 25th Sagamore Army Materials Research Conf., Bolton Landing, Lake George, N.Y., U.S.A., July 17-21, (1978), pp. 1-39.

(4) A. Kelly and R.B. Nicholson: "Precipitation-Hardening", Progress in Mat. Sci., 10, 3 (1963), pp. 151-391.

(5) S.H. Reichman and J.W. Smith: "Superplasticity in P/M In-100 Alloy", Int. J. of Powder Metallurgy, 6, 1, (1970), pp. 65-75.